

# SHAPE PHASE TRANSITIONS AND RANDOM INTERACTIONS

Roelof BIJKER

*ICN-UNAM, AP 70-543, 04510 México, DF, México*

The phenomenon of emerging regular spectral features from random interactions is addressed in the context of the interacting boson model. A mean-field analysis links different regions of the parameter space with definite geometric shapes. The results provide a clear and transparent interpretation of the high degree of order that has been observed before in numerical studies.

## 1 Introduction

Recent shell model calculations for even-even nuclei in the *sd* shell and the *pf* shell showed, despite the random nature of the two-body matrix elements, a remarkable statistical preference for ground states with angular momentum  $L = 0$ <sup>1</sup>. A similar dominance of  $L = 0$  ground states was found in an analysis of the Interacting Boson Model (IBM) with random interactions<sup>2</sup>. In addition, in the IBM there is strong evidence for both vibrational and rotational band structures. According to the conventional ideas in the field, the occurrence of regular spectral features is due to a very specific form of the interactions. The studies with random interactions show that the class of Hamiltonians that lead to these ordered patterns is much larger than is usually thought.

The basic ingredients of the numerical simulations, both for the nuclear shell model and for the IBM, are the structure of the model space, the ensemble of random Hamiltonians, the order of the interactions (one- and two-body), and the global symmetries, i.e. time-reversal, hermiticity and rotation and reflection symmetry. The latter three symmetries of the Hamiltonian cannot be modified, since we are studying many-body systems whose eigenstates have real energies and good angular momentum and parity. It was found that the observed spectral order is a rather robust property which does not depend on the specific choice of the (two-body) ensemble of random interactions<sup>1,3,4,5</sup>, the time-reversal symmetry<sup>3</sup>, or the restriction of the Hamiltonian to one- and two-body interactions<sup>6</sup>. This suggests that that an explanation of the origin of the observed regular features has to be sought in the many-body dynamics of the model space and/or the general statistical properties of random interactions.

The purpose of this contribution is to investigate the distribution of ground state angular momenta for the IBM in a Hartree-Bose mean-field analysis<sup>7</sup>.

## 2 Phase transitions

The IBM describes low-lying collective excitations in nuclei in terms of a system of  $N$  interacting quadrupole ( $d^\dagger$ ) and monopole ( $s^\dagger$ ) bosons<sup>8</sup>. The IBM Hamiltonian spans a wide range of collective features which includes vibrational, rotational and  $\gamma$  unstable nuclei. The connection with potential energy surfaces, geometric shapes and phase transitions can be studied by means of Hartree-Bose mean-field methods<sup>9,10</sup> in which the trial wave function is written as a coherent state. For one- and two-body interactions the coherent state can be expressed in terms of an axially symmetric condensate

$$|N, \alpha\rangle = \frac{1}{\sqrt{N!}} \left( \cos \alpha s^\dagger + \sin \alpha d_0^\dagger \right)^N |0\rangle , \quad (1)$$

with  $-\pi/2 < \alpha \leq \pi/2$ . The angle  $\alpha$  is related to the deformation parameters in the intrinsic frame,  $\beta$  and  $\gamma$ <sup>9</sup>. First we investigate the properties of some schematic Hamiltonians that have been used in the study of shape phase transitions.

### 2.1 The $U(5)$ - $SO(6)$ case

The transition from vibrational to  $\gamma$  unstable nuclei can be described by the Hamiltonian

$$H = \frac{\cos \chi}{N} d^\dagger \cdot \tilde{d} + \frac{\sin \chi}{4N(N-1)} (s^\dagger s^\dagger - d^\dagger \cdot d^\dagger) (\tilde{s} \tilde{s} - \tilde{d} \cdot \tilde{d}) , \quad (2)$$

which exhibits a second order phase transition at  $\chi_c = \pi/4$ <sup>9</sup>. For the present application, we extend the range of the angle  $\chi$  to that of a full period  $-\pi/2 < \chi \leq 3\pi/2$ , so that all possible combinations of attractive and repulsive interactions are included. The potential energy surface is given by the expectation value of  $H$  in the coherent state

$$E(\alpha) = \cos \chi \sin^2 \alpha + \frac{1}{4} \sin \chi \cos^2 2\alpha . \quad (3)$$

The equilibrium configurations are characterized by the value of  $\alpha = \alpha_0$  for which the energy surface has its minimum. They can be divided into three different classes or shape phases

$$\begin{array}{ll} \alpha_0 = 0 & -\pi/2 < \chi \leq \pi/4 \\ \cos 2\alpha_0 = \cot \chi & \pi/4 \leq \chi \leq 3\pi/4 \\ \alpha_0 = \pi/2 & 3\pi/4 \leq \chi \leq 3\pi/2 \end{array} \quad (4)$$

which correspond to an *s*-boson or spherical condensate, a deformed condensate, and a *d*-boson condensate, respectively. The phase transitions at the critical points  $\chi_c = \pi/4$  and  $3\pi/4$  are of second order, whereas the one at  $3\pi/2$  is of first order.

The angular momentum of the ground state can be obtained from the rotational structure of the equilibrium configuration, in combination with the Thouless-Valatin formula for the corresponding moments of inertia<sup>10</sup>.

- For  $\alpha_0 = 0$  the equilibrium configuration has spherical symmetry, and hence can only have  $L = 0$ .
- For  $0 < \alpha_0 < \pi/2$  the condensate is deformed. The ordering of the rotational energy levels  $L = 0, 2, \dots, 2N$

$$E_{\text{rot}} = \frac{1}{2\mathcal{I}_3} L(L+1) , \quad (5)$$

is determined by the sign of the moment of inertia

$$\mathcal{I}_3 = \frac{3N(\sin \chi - \cos \chi)}{\sin \chi \cos \chi} . \quad (6)$$

For  $\pi/4 \leq \chi \leq \pi/2$  the moment of inertia  $\mathcal{I}_3$  is positive and hence the ground state has angular momentum  $L = 0$ , whereas for  $\pi/2 \leq \chi \leq 3\pi/4$  it is negative corresponding to a ground state with  $L = 2N$ .

- For  $\alpha_0 = \pi/2$  we find a condensate of  $N$  quadrupole or *d*-bosons, which corresponds to a quadrupole oscillator with  $N$  quanta. Its rotational structure is characterized by the labels  $\tau$ ,  $n_\Delta$  and  $L$ . The boson seniority  $\tau$  is given by  $\tau = 3n_\Delta + \lambda = N, N-2, \dots, 1$  or 0 for  $N$  odd or even, and the values of the angular momenta are  $L = \lambda, \lambda+1, \dots, 2\lambda-2, 2\lambda$ <sup>8</sup>. In general, the rotational excitation energies depend on two moments of inertia

$$E_{\text{rot}} = \frac{1}{2\mathcal{I}_5} \tau(\tau+3) + \frac{1}{2\mathcal{I}_3} L(L+1) . \quad (7)$$

For the special case of the Hamiltonian of Eq. (2) only the first term is present

$$\mathcal{I}_5 = -\frac{2N}{\sin \chi} . \quad (8)$$

For  $3\pi/4 \leq \chi \leq \pi$  the moment of inertia  $\mathcal{I}_5$  is negative and the ground state has  $\tau = N$ , whereas for  $\pi \leq \chi \leq 3\pi/2$  it is positive and the ground state has  $\tau = 0$  ( $L = 0$ ) for  $N$  even, and  $\tau = 1$  ( $L = 2$ ) for  $N$  odd.

In Fig. 1 we compare the percentages of ground states with  $L = 0$  and  $L = 2$  as a function of  $N$  obtained exactly (solid lines) and in the mean-field

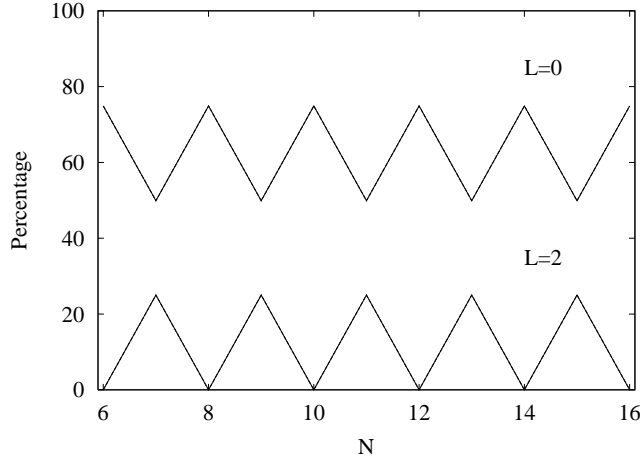


Figure 1: Percentages of ground states with  $L = 0$  and  $L = 2$  for the schematic IBM Hamiltonian of Eq. (2) with  $-\pi/2 < \chi \leq 3\pi/2$  calculated exactly (solid lines) and in mean-field approximation (dashed lines).

analysis (dashed lines). The results were obtained by assuming a constant probability distribution for  $\chi$  on the interval  $-\pi/2 < \chi \leq 3\pi/2$ . We have added a small attractive  $\vec{L} \cdot \vec{L}$  interaction to remove the degeneracy of the ground state for the  $\tau = N$  solution. There is a perfect agreement for all values of  $N$ . The ground state is most likely to have angular momentum  $L = 0$ : in 75% of the cases for  $N$  even and in 50% for  $N$  odd. In 25% of the cases, the ground state has the maximum value of the angular momentum  $L = 2N$ . The only other value that occurs is  $L = 2$  in 25% of the cases for  $N$  odd. The oscillation in the  $L = 0$  and  $L = 2$  percentages is due to the contribution of the  $d$ -boson condensate. The sum of the  $L = 0$  and  $L = 2$  percentages is constant (75%) and does not depend on  $N$ .

## 2.2 The $U(5)$ - $SU(3)$ case

A second transitional region of interest is the one between vibrational and rotational nuclei. In the IBM, it can be described schematically by

$$H_{\pm} = \cos \chi d^{\dagger} \cdot \tilde{d} + \frac{\sin \chi}{N-1} \left[ (2s^{\dagger} \cdot s^{\dagger} - d^{\dagger} \cdot d^{\dagger}) (2\tilde{s} \cdot \tilde{s} - \tilde{d} \cdot \tilde{d}) + (2s^{\dagger} \times d^{\dagger} \pm \sqrt{7}d^{\dagger} \times d^{\dagger})^{(2)} \cdot (2\tilde{d} \times \tilde{s} \pm \sqrt{7}\tilde{d} \times \tilde{d})^{(2)} \right]. \quad (9)$$

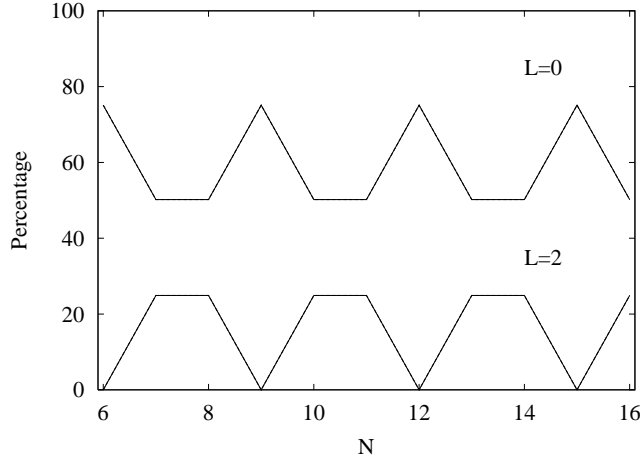


Figure 2: As Fig. 1, but for the schematic IBM Hamiltonian of Eq. (9).

In the physical region  $0 \leq \chi \leq \pi/2$ ,  $H_{\pm}$  exhibits a first order phase transition at  $\chi_c = \arctan 1/9^9$ . As before, here we consider the interval  $-\pi/2 < \chi \leq 3\pi/2$ . The results for the distribution of ground state angular momenta are presented in Fig. 2. For  $N = 3k$  the ground state has  $L = 0$  in 75% of the cases and  $L = 2N$  in the remaining 25%. For  $N = 3k + 1$  and  $N = 3k + 2$  the ground state angular momentum is either  $L = 0$  (50%),  $L = 2$  (25%) or  $L = 2N$  (25%). The variation in the  $L = 0$  and  $L = 2$  percentages is due to the contribution of the  $d$ -boson condensate, whereas the sum of the two is constant (75%).

### 2.3 The $SU(3)$ - $SO(6)$ case

The transitional region between rotational and  $\gamma$  unstable nuclei described by the Hamiltonian

$$\begin{aligned}
 H_{\pm} = & \frac{\cos \chi}{4(N-1)} (s^{\dagger} \cdot s^{\dagger} - d^{\dagger} \cdot d^{\dagger}) (\tilde{s} \cdot \tilde{s} - \tilde{d} \cdot \tilde{d}) \\
 & + \frac{\sin \chi}{N-1} \left[ (2s^{\dagger} \cdot s^{\dagger} - d^{\dagger} \cdot d^{\dagger}) (2\tilde{s} \cdot \tilde{s} - \tilde{d} \cdot \tilde{d}) \right. \\
 & \left. + (2s^{\dagger} \times d^{\dagger} \pm \sqrt{7}d^{\dagger} \times d^{\dagger})^{(2)} \cdot (2\tilde{d} \times \tilde{s} \pm \sqrt{7}\tilde{d} \times \tilde{d})^{(2)} \right], \quad (10)
 \end{aligned}$$

does not show a phase transition in the physical region  $0 \leq \chi \leq \pi/2^9$ . Fig. 3 shows that the distribution of the ground state angular momenta is very similar to the previous case.

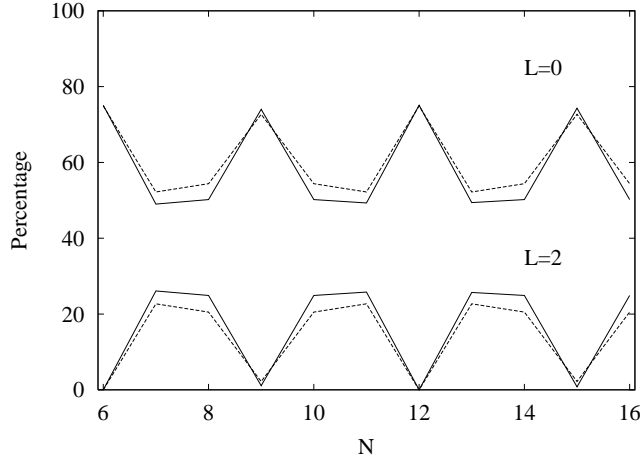


Figure 3: As Fig. 1, but for the schematic IBM Hamiltonian of Eq. (10).

### 3 Random interactions

Finally, we apply the mean-field analysis to the general one- and two-body IBM Hamiltonian

$$H = \frac{1}{N} \left[ H_1 + \frac{1}{N-1} H_2 \right], \quad (11)$$

in which the nine parameters of this Hamiltonian are taken as independent random numbers on a Gaussian distribution with zero mean and width  $\sigma$ . The distribution of geometric shapes for this ensemble of Hamiltonians is determined by the distribution of equilibrium configurations of the corresponding potential energy surfaces

$$E(\alpha) = a_4 \sin^4 \alpha + a_3 \sin^3 \alpha \cos \alpha + a_2 \sin^2 \alpha + a_0. \quad (12)$$

The coefficients  $a_i$  are linear combinations of the Hamiltonian parameters. The spectral properties of each Hamiltonian of the ensemble of random one- and two-body interactions are analyzed by exact numerical diagonalization<sup>2</sup> and by mean-field analysis<sup>7</sup>.

In Fig. 4 we compare the percentages of  $L = 0$  and  $L = 2$  ground states obtained exactly (solid lines) and in the mean-field analysis (dashed lines). There is a dominance of ground states with  $L = 0$  for  $\sim 63 - 77\%$  of the cases. For  $N = 3k$  we see an enhancement for  $L = 0$  and a corresponding decrease

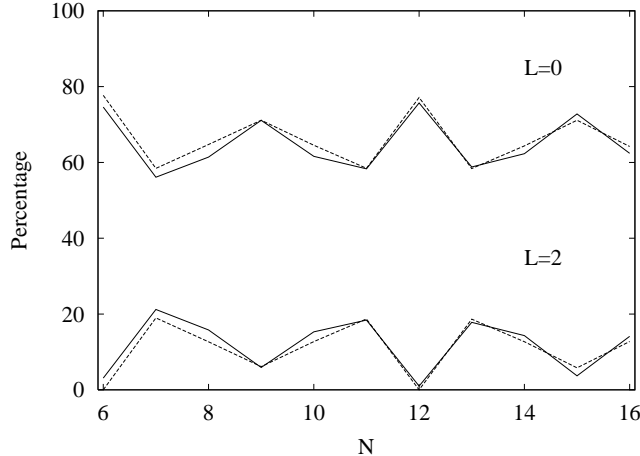


Figure 4: As Fig. 1, but for the random IBM Hamiltonian of Eq. (11).

for  $L = 2$ . Also in this case, the equilibrium configurations can be divided into three different classes: an  $s$ -boson or spherical condensate, a deformed condensate, and a  $d$ -boson condensate. For the spherical and deformed solutions the ground state has  $L = 0$  ( $\sim 63\%$ ) or  $L = 2N$  ( $\sim 13\%$ ). The analysis of the  $d$ -boson condensate is a bit more complicated due to the presence of two moments of inertia,  $\mathcal{I}_5$  and  $\mathcal{I}_3$ . There is a constant contribution to  $L = 2N$  ground states ( $\sim 10\%$ ), whereas the  $L = 0$  and  $L = 2$  percentages show oscillations with  $N^7$ . Just as for the schematic Hamiltonians, the sum of the  $L = 0$  and  $L = 2$  percentages is constant and independent of  $N$ .

#### 4 Summary and conclusions

In this contribution, we have investigated the origin of the regular features that have been observed in numerical studies of the IBM with random interactions, in particular the dominance of ground states with  $L = 0$ .

In a mean-field analysis, it was found that different regions of the parameter space can be associated with particular intrinsic vibrational states, which in turn correspond to definite geometric shapes: a spherical shape, a deformed shape or a condensate of quadrupole bosons. An analysis of the angular momentum content of each one of the corresponding condensates combined with the sign of the relevant moments of inertia, provides an explanation for the distribution of ground state angular momenta of both schematic and random

forms of the IBM Hamiltonian.

In summary, the present results show that mean-field methods provide a clear and transparent interpretation of the regular features that have been obtained before in numerical studies of the IBM with random interactions. The same conclusions hold for the vibron model<sup>11</sup>. For the nuclear shell model the situation is less clear. Despite the large number of studies that have been carried out to explain and/or further explore the properties of random nuclei no definite answer is yet available<sup>12</sup>.

### Acknowledgments

It is a great pleasure to dedicate this contribution to the 60th birthday of Jerry P. Draayer. Congratulations, Jerry! This work was supported in part by CONACyT under project No. 32416-E.

1. C.W. Johnson, G.F. Bertsch and D.J. Dean, Phys. Rev. Lett. **80**, 2749 (1998).
2. R. Bijker and A. Frank, Phys. Rev. Lett. **84**, (2000), 420.
3. R. Bijker, A. Frank and S. Pittel, Phys. Rev. C **60**, 021302 (1999).
4. C.W. Johnson, G.F. Bertsch, D.J. Dean and I. Talmi, Phys. Rev. C **61**, 014311 (2000).
5. D. Dean, Nucl. Phys. A **682**, 194c (2001).
6. R. Bijker and A. Frank, Phys. Rev. C **62**, 014303 (2000).
7. R. Bijker and A. Frank, Phys. Rev. C **64**, 061303 (2001).
8. F. Iachello and A. Arima, *The interacting boson model* (Cambridge University Press, 1987).
9. A.E.L. Dieperink, O. Scholten and F. Iachello, Phys. Rev. Lett. **44**, 1747 (1980); A.E.L. Dieperink and O. Scholten, Nucl. Phys. A **346**, 125 (1980).
10. J. Dukelsky, G.G. Dussel, R.P.J. Perazzo, S.L. Reich and H.M. Sofia, Nucl. Phys. A **425**, 93 (1984).
11. R. Bijker and A. Frank, Phys. Rev. C **65**, 044316 (2002).
12. see e.g. R. Bijker and A. Frank, Nuclear Physics News, Vol. **11**, No. 4, 15 (2001); V.G. Zelevinsky, D. Mulhall and A. Volya, Phys. Atom. Nucl. **64**, 525 (2001).